Statistical Analysis of Interference Between Earth Stations and Ear[h-Orbiting Satellites

Dennis F. Bishop, *Member, IEEE*

Abstract - Determination of the potential for radio frequency interference between Earth stations and orbiting spacecraft is often desirable. This information can be used to select frequencies for radio systems to avoid interference or it can be used to determine if coordination between radio systems is necessary. Also, it is useful for planning emission standards and filtering requirements for future telecommunications equipment, A mode] is developed that will determine the statistics of interference between Earth stations and elliptical orbiting spacecraft. The model uses orbital dynamics, detailed antenna patterns, and spectral characteristics to obtain accurate levels of interference at the victim receiver. The model is programmed into a computer simulation to obtain long term statistics of interference. An example is shown to demonstrate the model. Interference from Earth exploration-satellites to a deep space Earth station is simulated. A second example of interference from a fixed-satellite Earth station to an orbiting scatterometer receiver is left for a future paper.

1. Introduction

Fig. 1 contains an illustration of the interference geometry for Earth orbiters and an Earth station. Spacecraft 1 may be transmitting or receiving. Its antenna is pointed toward an arbitrary location on Earth. The Earth station may be transmitting or receiving. Its antenna is pointed toward spacecraft 2 or toward an arbitrary point described by the Earth station antenna azimuth and elevation.

Two interference scenarios are considered. in the first scenario the Earth station is transmitting a signal toward spacecraft 2. This signal is unintentionally received by spacecraft 1. In the second scenario spacecraft 1 is transmitting a signal that is unintentionally received by the Earth station. The Earth station is pointed toward an arbitrary location described by antenna azimuth and elevation.

2. interference Geometry and Orbital Dynamics Models

The interference geometry shown in Fig. 1 is common to many interference scenarios that occur between two different radio systems. The level of interference that occurs at a victim receiver depends on angles γ_g and γ_{rg} and the distance D_{sf} that are shown in Fig. 1. The interference angles and path distance in Fig. 1 may be computed with standard orbit determination methods [1]. The spacecraft orbit plane is illustrated in Fig. 2. The position of spacecraft 1 is computed first,

$$x_w = (a[\cos(E)]-ae,\ a[1-e^2]^{1/2}[\sin(E)],\ 0)^T = (x_w,\ y_w,\ z_w)^T \qquad (1)$$

where

a = semi-major axis (Earth radii)
E = eccentric anomally (radians)
M = E - e(sin[E]) = mean anomally (radians)
= nt
e = orbit eccentricity
n = 0.07437 / $a^{3/2}$ (radians / minute)
t = time (minutes)

Newton's iteration [2] may be used to solve for the eccentric anomally.

$$E_0 = M + e(\sin[M])/(1-\sin[M+e]+\sin[M]) \quad (2)$$
$$M_k = E_k - e(\sin[E_k])$$
$$E_{k+1} = E_k - t\,(M-M_k)/(1-e\,[\cos(E_k)]$$

where

k = o, 1, 2, . . .

The position of spacecraft 1 in the orbit plane is converted to position in the right ascension-declination coordinate system.

$$x = \mathbf{P}x_w = (x,y,z)^T \quad \textbf{(3)}$$

where

$$\boldsymbol{P} = \begin{bmatrix} P_x & Q_x & W_x \\ P_y & Q_y & W_y \\ P_z & Q_z & W_z \end{bmatrix}$$

P_x = C O C O S - sin(ω)sin(Ω)cos(i)
P_y = cos(ω)sin(Ω) + sin(ω)cos(Ω)cos(i)
P_z = sin(ω) sin(i)
Q_x = -sin(0) cos(Ω) - cos(ω)sin(Ω)cos(i)
Q_y = -sin(ω)sin(Ω) + cos(ω)cos(Ω)cos(i)
Q_z = c o u s i n
W_x = sin(Ω)sin(i)
WY = -cos(Ω)sin(i)
W_z = cos(i)
ω = argument of perigee
Ω = longitude of the ascending node
i = orbital inclination

The location of the Earth station is determined in the right ascension-declination coordinate system.

$$\mathbf{x}_g = (\sin[\theta]\cos[\phi], \sin[\theta]\sin[\phi], \cos[\theta])^T = (x_g, y_g, z_g)^T \quad (4)$$

where

$\theta = 90 - l_a$
$\phi = l_o + k + 360t/1436.1$
k = an arbitrary constant used to rotate the Earth station relative to the orbit plane (degrees)
l_a = Earth station latitude (degrees)
l_0 = Earth station longitude (degrees)

The Earth station may be pointed at another satellite (spacecraft 2) or its boresight direction may be described with azimuth and elevation notation. If it is pointed" at spacecraft 2, that satellite's position may be described with (1-3), with a different value for n.

$$\mathbf{x}_2 = (x_2, y_2, z_2)^T \quad (5)$$

A special case exists when spacecraft 2 is in a geostationary orbit. It may be assumed that spacecraft 2 is located in the equator plane. The location is determined in the right ascension-declination coordinate system.

$$X_2 = \mathbf{x}_{gs} = 6.6257\,(\sin[\theta_g]\cos[\phi_g], \sin[\theta_g]\sin[\phi_g], 0)^T \quad (6)$$

where

$\theta_g = 90$
ϕ_g = geostationary longitude + k + $360t/1436.1$

If the Earth station is pointed at a specific elevation and azimuth then the boresight direction of the Earth station may be converted from azimuth, elevation coordinates to Earth-centered coordinates.

$$\mathbf{x}_{ec} = \mathbf{C}\mathbf{x}_{ae} = (x_{ec}, y_{ec}, z_{ec})^T \quad (7)$$

where

$$C = \begin{bmatrix} C_1 & C_2 & C_3 \\ C_4 & C_5 & C_6 \\ C_7 & C_8 & C_9 \end{bmatrix}$$

$C_1 = \cos(l_o)\cos(90\text{-}l_a)$
$C_2 = -\cos(90\text{-}l_o)$
$C_3 = \cos(l_a)\cos(l_o)$
$C_4 = \mathrm{COS}(90\text{-}1_0)\mathrm{COS}(90\text{-}1J$
$C_5 = \cos(l_o)$
$C_6 = \mathrm{COS}(1,)\mathrm{COS}(90\text{-}1_0)$
$C_7 = -\cos(l_a)$
$C_8 = 0$
$C_9 = \cos(90\text{-}l_a)$

$\mathbf{x}_{ae} = (-\cos[el]\cos[az], \cos[el]\sin[az], \sin[el])^T$

el = elevation of Earth station antenna
az = azimuth of Earth station antenna

These coordinates are converted to spherical coordinates.

$$\theta_b = \cos^{-1}(z_{ec}/r_{ec}) \text{ (degrees)} \quad \textbf{(8)}$$
$$\phi_b = \cos^{-1}(x_{ec}/r_{xy}) + k + 360t/1436.1\,,\ y_{ec} \geq 0 \text{ (degrees)}$$
$$= \mathbf{360}\text{-}\ \cos^{-1}(x_{ec}/r_{xy}) + k + 360t/1436.1,\ y_{ec} < 0$$

where

$r_{ec} = (x_{ec}^2 + y_{ec}^2 + z_{ec}^2)^{1/2}$
$r_{xy} = (x_{ec}^2 + y_{ec}^2)^{1/2}$

Finally, these coordinates are converted to the right ascension-declination coordinate system.

$$\mathbf{x}_{bor} = r_{ec}(\sin[\theta_b]\cos[\phi_b], \sin[\theta_b]\sin[\phi_b], \cos[\theta_b])^T \quad \textbf{(9)}$$

The line-of-sight visibility of the Earth station to spacecraft 1 is determined. Fig. 3 illustrates the central angle between the two. The central angle between spacecraft 1 and the Earth station is computed.

$$x \bullet \mathbf{x}_g = |\mathbf{x}|\cos(\gamma) \quad \text{(lo)}$$

Fig. 3 also illustrates the limit of visibility. The constraint is that the line between spacecraft 1 and the Earth station is tangent to the Earth. Central angles that are less than or equal to this angle indicate that spacecraft 1 is visible to the Earth station.

$$\gamma_v = \cos^{-1}(1 / |\mathbf{x}_v|) \tag{11}$$

The visibility condition is stated.

$$\gamma \le \gamma_v \tag{12}$$

Interference between spacecraft 1 and the Earth station can occur only if they are visible. If spacecraft 1 is visible then additional computations are necessary. The angle, γ_{rg}, on Fig. 1 is used to compute the antenna gain of the Earth station in the direction of spacecraft 1. The vector from the Earth station to spacecraft 2 is computed.

$$\mathbf{x}_{fg} = \mathbf{x}_2 - \mathbf{x}_g \tag{13}$$

A special case occurs when spacecraft 2 is a geostationary satellite:

$$\mathbf{x}_2 = \mathbf{x}_{gs} \tag{14}$$

If the pointing of the Earth station antenna is described in terms of azimuth and elevation then:

$$\mathbf{x}_{fg} = \mathbf{x}_{bor} \tag{15}$$

The vector from the Earth station to spacecraft 1 is computed.

$$\mathbf{x}_{fs} = \mathbf{x} - \mathbf{x}_g \tag{16}$$

The angle between these two vectors (13, 16) can be used to determine the antenna gain of the Earth station in the direction of spacecraft 1.

$$\mathbf{x}_{fg} \bullet \mathbf{x}_{fs} = |\mathbf{x}_{fg}||\mathbf{x}_{fs}|\cos(\gamma_{rg}) \tag{17}$$

The International Telecommunication Union (ITU) antenna pattern is used to calculate the Earth station antenna gain [3].

$$\begin{aligned} G(\gamma_{rg}) &= G_p - 2.5\times10^{-3}(D\gamma_{rg}/\lambda)^2 && \text{(dBi)}, 0^\circ \le \gamma_{rg} < \phi_m \\ &= G_1 && , \phi_m \le \gamma_{rg} < \phi_r \\ &= 32 - 25\log(\gamma_{rg}) && , \phi_r \le \gamma_{rg} < 48^\circ \\ &= -10 && , 48^\circ \le \gamma_{rg} < 180^\circ \end{aligned} \tag{18}$$

where

G_p = peak antenna gain (dBi)
D = antenna diameter (meters)
λ = wavelength (meters) = c/f
$G_1 = 2 + 15\log(D/\lambda)$ (dBi)
$\phi_{m1} = 20\lambda(G_p - G_1)^{1/2}/D$ (degrees)
$\phi_r = 15.85(D/\lambda)^{-0.6}$ (degrees)
c = speed of light = 3×10^8 m/s
f = frequency (Hz)

This equation is valid for $D/\lambda \geq 100$. A different antenna pattern is used for D/λ c 100 [3].

The distance between the the Earth station and spacecraft 1 is computed.

$$D_{sf} = 6378 |\mathbf{x}_g - \mathbf{x}| \text{(km)} \tag{19}$$

Then, the path loss between the two points is computed.

$$PL = 20\log(c/[4\pi D_{sf} f]) \text{(dB)} \tag{20}$$

The angle, γ_g, on Fig. 1 is used to compute the antenna gain of spacecraft 1 in the direction of the Earth station.

$$\mathbf{x}_{b1} \bullet (-\mathbf{x}_{fs}) = |\mathbf{x}_{b1}| \, |\mathbf{x}_{fs}| \cos(\gamma_g) \tag{21}$$

where

$\mathbf{x}_{b1}$ = boresight vector of spacecraft 1 antenna

A special case occurs when the antenna of spacecraft 1 points toward the center of the Earth.

$$\mathbf{x}_{b1} = -\mathbf{x} \tag{22}$$

3. Application: Simulation of Interference from an Earth Exploration-Satellite to a Deep Space Earth Station

The Deep Space Network (DSN) uses the 8400- to 8450-MHz band for space-to-Earth transmissions. The Earth station receivers are protected by interference criteria that have been negotiated in international forums [4, 5]. Other radio services that use the 8400- to 8450-MHz band are aware of the interference criteria and limit their transmissions accordingly. However, radio services that transmit in bands that are adjacent to the DSN bands may not be fully aware of their emissions in the DSN band. If" these out-of-band emissions are strong enough they can disrupt DSN communications. This section

investigates some of the low Earth orbiting spacecraft that transmit in bands that arc adjacent to the DSN bands near 8400 MHz.

The Earth cx}>loratiol~-satellite' service has an allocation to use the 8175- to 8400-MHz band [6] for transmissions in the space-to-Earth direction, Typically, these satellites are in orbits below 1000 km and use high data rate QPSK modulation formats. Unless proper filtering is used these spacecraft can produce spectral components that disrupt deep space communications in the DSN band.

The Space Frequency Coordination Group (SFCG) is an informal international organization of space agencies that have an interest in space research, remote sensing by satellite, meteorological satellites, inter-satellite links, and radioastronorny [7]. These agencies meet on an annual basis to agree on frequency management policies and practices that protect and enhance their common interest. An output of the group is the Handbook of the SFCG which contains resolutions and recommendations that direct spectrum policy among these agencies, All SFCG work is in harmony with the International Telecommunications Union (ITU) Radio Regulations [3, 6]. One current topic of study for the SFCG is the problem of adjacent band interference from low Earth orbiters to the DSN Earth station receivers near 8.4 GHz. The models developed in this paper are used to determine the susceptibility of the DSN and recommend emission standards for low Earth orbiters,

3.1 Worst-Case Power Spectral Density (Ideal Data Waveform) of Adjacent Band Interferers

Table 1 contains a list of some spacecraft that transmit in frequency bands that are adjacent to the deep space (space-to-Earth) downlinks at 8400-8450 MHz [8, 9]. Fig. 4 contains a plot of the power spectral density of the Earth Observing System (EOS) spacecraft transmitting in the direct broadcase (DB) mode (QPSK, 30 MBPS per channel). The power spectral density is computed with the following equation:

$$P_{SD} = P_T + SD(f) + G_T + PL_1 + G_R \qquad \textbf{(23)}$$

where

P_{SD} = power spectral density of interfering spacecraft at deep space Earth station receiver (dBW/Hz)
P_1 = spacecraft transmitter power (dBW)
SD(f) = spectral density of spacecraft transmitter (Table II) (dB/Hz)
G_T = peak transmit antenna gain (dBi)
PL_1 = path loss (dB)
$= 20\log[c/(4\pi A_m f)]$
c = speed of light = $3x10^5$ km / s
A_m = minimum orbit altitude (km)

f = frequency (Hz)
G_R = DSN receive antenna gain = 74 dBi

The spectral density is computed from the equations shown in Table 11 [1 O, 11], Fig. 4 shows that the emission of the EOS spacecraft_ exceeds the DSN interference criterion by about 45 dB in the 8400- to 8450-MHz band. Table III contains a list of some adjacent band spacecraft and the amount that their emissions exceed (ideal data waveform column) the DSN interference criterion in the 8400- to 8450-MHz band. Equation (23) produces a worst-case power spectral density at the deep space Earth station because peak antenna gains are used and the minimum orbit altitude is used to compute the path loss.

3.2. **The Effect of Data Asymmetry and Finite Transition Time on the Power Spectral Density**

The power spectral density of asymmetric NRZ data has been derived [12]. The baseband waveform of asymmetric NRZ data maybe represented with the 4-ary source shown on Fig, 5. The baseband signals shown on Fig. 5 have the following equations:

$$g_1(t) = A\ ,\ -T/2 \le t \le T(1+\Delta)/2 \qquad (24)$$

$$= O\ ,\ \text{elsewhere}$$

$$g_2(t) = -A\ ,\ -T/2 \le t \le T(1-\Delta)/2$$

$$= O\ ,\ \text{elsewhere}$$

$$g_3(t) = A\ ,\ -T/2 \le t \le T/2$$

$$= O\ ,\ \text{elsewhere}$$

$$g_4(t) = -A\ ,\ -T/2 \le t \le T/2$$

$$= O\ ,\ \text{elsewhere}$$

where

t = time (seconds)
A = height of pulse
T = length of normal pulse
A/2 = data asymmetry

The Fourier transforms of these four signals may be described by the following equations:

$$G_1(f) = A\exp(-j\pi fT\Delta/2)\sin(\pi fT[1+A/2])/(\pi f) \quad (25)$$

$$G_2(f) = -A\exp(j\pi fT\Delta/2)\sin(\pi fT[1-\Delta/2])/(\pi f)$$

$$G_3(f) = A\sin(\pi fT)/(\pi f)$$

$$G_4(f) = -G_3(f)$$

where

f = frequency (Hz)
$j = (-1)^{1/2}$

The discrete power spectral density is determined with the following equation [12]:

$$S_d(f) = T^{-2}|p_1G_1(0)+p_2G_2(0)+p_3G_3(0)+p_4G_4(0)|^2\delta(f) + \quad (26)$$

$$2\,T^{-2}\sum_{n=1}^{\infty}|p_1G_1(n/T)+p_2G_2(n/T)+p_3G_3(n/T)+p_4G_4(n/T)|^2\,\delta(f-n/T)$$

where

$p_1 = pp_t$
$p_2 = (1-p)p_t$
$p_3 = p(1-p_t)$
$p_4 = (1-p)(1-p_t)$
p = probability of transmitting a positive pulse
p_t = transition density

The values of the functions in (25) at zero frequency (f = O) are equal to the areas under the time functions [13].

$$G_1(0) = AT(1+\Delta/2) \quad (27)$$

$$G_2(O) = -AT(1-A/2)$$

$$G_3(0) = AT$$

$$G_4(O) = -AT$$

The values of the functions in (25) at integral multiples of the data rate (f = n/T) may be determined,

$$G_1(n/T) = A\exp(-j\pi n\Delta/2)\sin(\pi n[1-t\,\Delta/2])/(\pi n/T) \quad (28)$$

$$G_2(n/T) = -A\exp(j\pi n\Delta/2)\sin(\pi n[1-\Delta/2])/(\pi n/T)$$

$$G_3(f) = o$$

$$G_4(f) = o$$

The continuous power spectral density is determined with the following equation [12]:

$$S_c(f) = T^{-1}[p_1(1-p_1)|G_1(f)|^2 + p_2(1-p_2)|G_2(f)|^2 + p_3(1-p_3)|G_3(f)|^2 + p_4(1-p_4)|G_4(f)|^2] \quad (29)$$

$$-2T^{-1}(p_1p_2\mathrm{Re}[G_1(f)G_2^*(f)] + p_1p_3\mathrm{Re}[G_1(f)G_3^*(f)] + p_1p_4\mathrm{Re}[G_1(f)G_4^*(f)] +$$

$$p_2p_3\mathrm{Re}[G_2(f)G_3^*(f)] + p_2p_4\mathrm{Re}[G_2(f)G_4^*(f)] + p_3p_4\mathrm{Re}[G_3(f)G_4^*(f)])$$

Fig. 6 illustrates the finite transition time.

$$T_t = T\gamma/2 \quad (30)$$

where

T_t = transition time (seconds)

The transition time is modelled with a first-order Butterworth filter. The filter bandwidth determines the transition time. The discrete and continuous spectra of (26, 29) are multiplied by the magnitude squared of the filter response.

$$S_d'(f) = S_d(f)|H_B(f)|^2 \quad (31)$$

$$SC'(f) = SC(f)|H_B(f)|^2$$

where

$|H_B(f)|^2$ = frequency response of Butterworth filter

$$= [1+(f/f_{3db})^{2m}]^{-1}$$

where

f_{3db} = 3 dB filter bandwidth
m = filter order, $m \geq 1$

The time response of the first-order filter o the perfect transition shown on Fig. 6 may be determined [14].

$$r(t') = A(2\exp[-2\pi f_{3db}t']-1),\ t' \geq 0 \tag{32}$$

where

$$t' = t - T/2$$

Arbitrarily, the transition time is selected to be the time where the response is 95% of the final value. The filter bandwidth as a function of transition time can be determined from (30, 32).

$$f_{3db} = [\ln([1-0.95]/2)] / (-2\pi T_r) \tag{33}$$

When the baseband NRZ signal is carrier modulated the PSD takes the following form [15]:

$$S_{ca}(f) = S_d'(f-f_c) + S,'(f-fc) \tag{34}$$

where

f_c = carrier frequency (Hz)

Fig. 7 shows a simple diagram of a QPSK modulator. The modulator inputs are asymmetric NRZ data streams. The PSD at the output of the modulator may be determined from the autocorrelation function of the time waveform.

$$ST(f) = \int_{-\infty}^{\infty} R_{XT}(\tau)\exp(-j2\pi f\tau)d\tau \tag{35}$$

where

$R_{XT}(\tau)$ = autocorrelation function of modulator output waveform

The autocorrelation function of this random process (stationarity assumed) is determined.

$$R_{XT}(\tau) = E[\{x_I(t)+x_Q(t)\}\{x_I(t+\tau)+x_Q(t+\tau)\}] \tag{36}$$

$$= E[x_I(t)x_I(t+\tau)] + E[x_Q(t)x_Q(t+\tau)]$$

$$+ E[x_I(t)x_Q(t+\tau)] + E[x_Q(t)x_I(t+\tau)]$$

$$= R_{XI}(\tau) + R_{XQ}(\tau)$$

$$+ E[x_I(t)x_Q(t+\tau)] + E[x_Q(t)x_I(t+\tau)]$$

The third term is examined in more detail.

$$E[x_I(t)x_Q(t+\tau)] = E[x_{Id}(t)\cos(\omega_c t)x_{Qd}(t+\tau)\sin(\omega_c[t+\tau])] \quad (37)$$

where

$x_{Id}(t)$ = I channel data

$x_{Qd}(t)$ = Q channel data

$\cos(\omega_c t)$ = carrier of I channel

$\sin(\omega_c t)$ = carrier of Q channel

The data terms are independent of the carrier terms. Therefore the expected value becomes the product of two expected value terms,

$$E[x_I(t)x_Q(t+\tau)] = E[x_{Id}(t)x_{Qd}(t+\tau)]\,E[\cos(\omega_c t)\sin(\omega_c[t+\tau])] \quad (38)$$
$$= E[x_{Id}(t)x_{Qd}(t+\tau)]\,E[\sin(\tau)+\sin(2\omega_c t+\tau)]/2$$

If the I channel data is independent of the Q channel data then further simplification is possible.

$$E[x_I(t)x_Q(t+\tau)] = E[x_{Id}(t)]\,E[x_{Qd}(t+\tau)]\,E[\sin(\tau)+\sin(2\omega_c t+\tau)]/2 \quad (39)$$

Using a similar argument, the last term in (36) may be derived.

$$E[x_Q(t)x_I(t+\tau)] = E[x_{Qd}(t)]\,E[x_{Id}(t+\tau)]\,E[-\sin(\tau)+\sin(2\omega_c t+\tau)]/2 \quad (40)$$

Then it is assumed that the expected value of the data streams does not depend on the starting location.

$$E[x_{Id}(t)] = E[x_{Id}(t+\tau)] \quad (41)$$

$$E[x_{Qd}(t)] = E[x_{Qd}(t+\tau)]$$

Combining (39, 40) yields the summation of the third and fourth terms in (36).

$$E[x_I(t)x_Q(t+\tau)] + E[x_Q(t)x_I(t+\tau)] = E[x_{Id}(t)]\,E[x_{Qd}(t)] \cdot \quad (42)$$
$$E[\sin(\tau)+\sin(2\omega_c t+\tau)-\sin(\tau)+\sin(2\omega_c t+\tau)]/2$$

$= 0$

Therefore the sum of the last two terms in (36) is zero and the output autocorrelation function of the QPSK modulator is the sum of the autocorrelation functions of each channel. Hence, the PSD of the output is the sum of the PSD of the I channel and the PSD of the Q channel.

$$S_{caqp}(f) = Sea,(f) + S_{caQ}(f) \tag{43}$$

where

$S_{cal}(f)$ = PSD of 1 channel (34)
$S_{caQ}(f)$ = PSD of Q channel (34)

A similar derivation can be performed to show that when the I channel data is identical to the Q channel data, (43) still applies.

Figs. 8-10 show plots of the power spectral density of the EOS spacecraft in the DB mode. The transition density (p_t) and the probability of transmitting a positive pulse (p) are set equal to 0.5. A 1 watt transmitter power is used. Table IV shows the data asymmetry and transition time parameters that are used in Figs. 8-10. Also, the level of the discrete component in the 8.4- to 8.45-GHz band is given. A l-Hz bandwidth is used for the discrete spectrum. A typical value of transition time for a high data rate system, e.g. the Tracking and Data Relay Satellite System [16], is about 5% of a bit time. When 5%. transition time is added to the 5% data asymmetry (Fig. 9) the discrete component is reduced 1.3 dB. This is due to the low pass filter effect of the transition time model. Much larger transition times would be required to substantially affect the level of the discrete component in the 8.4- to 8.45-GHz band. Fig. 10 shows the effect with a 50%/0 transition time. Here the discrete component in the 8.4 GHz band is reduced to an absolute level of -64.5 dBW/Hz (a 26.8 dB reduction relative to the component on Fig. 8). Table III shows the amount that the largest discrete component in the DSN band exceeds the DSN interference criterion for 0.05%, 0.5%, and 5% data asymmetry. The transition time is set equal to 0%, of a bit time. A 1-Hz bandwidth is used for the discrete tones. Equation (23) is used to compute the power spectral density at the DSN Earth station with the spectral density (SD(f)) determined with (34).

3.3. Simulation of Interference to a Deep Space Earth Station from Low Earth Orbiting Spacecraft in an Adjacent Band

It is useful to know the amount of time that the power spectral density from a spacecraft exceeds the interference criterion of the deep space Earth station. Fig. 11 shows a plot of satellite visibility to an Earth station versus orbit altitude. It is assumed that the satellite passes directly over the Earth station with a circular orbit. The geometry is illustrated in Fig. 12. The visibility time is computed.

$$T_{vis} = 3600 T_o \theta_v / \pi \text{ (seconds)} \quad (44)$$

where

T_o = orbital period (hours) [17]
$= 2\pi(A+R)^{3/2}/\mu^{1/2}$
A = orbit altitude (km)
R = Earth radius = 6378 km
μ = Earth gravitation, mass product
$= 5{,}17 \times 10^{12} km^3/hr^2$
θ_v = central angle (radians)
$= \cos^{-1}(R/[R+A])$

If the satellite has sufficient power it can produce line-of-sight interference to the Earth station during its orbit visibility time. This can be a significant amount of time even for a low altitude spacecraft. Interference times for actual spacecraft systems depend on transmitter power, orbits, antenna gains, etc. Fig. 1 can be used to illustrate the interference geometry. The low Earth orbit (LEO) spacecraft is represented with spacecraft 1. The deep space Earth station points at a specified azimuth and elevation. The 1 .EO spacecraft is in a circular orbit around the Earth with its antenna pointing toward the center of the Earth. The angle γ_{rg} between the antenna boresight of the deep space Earth station and the vector to the LEO spacecraft is computed with (15-17). The deep space Earth station (70 meter) antenna gain in the direction of the LEO spacecraft is computed with (18).

$$\begin{aligned} G_L(\gamma_{rg}) &= 74 - 0.0025(1960\gamma_{rg})^2 \text{ (dBi)}, && 0° \le \gamma_{rg} \text{ c } 0.0485° \\ &= 51.4 && 0.0485° \le \gamma_{rg} < 0.168° \\ &= 32 - 25\log(\gamma_{rg}) && :0{,}168° \le \gamma_{rg} < 48° \\ &= -lo && , 48° \le \gamma_{rg} \le 180° \end{aligned} \quad (45)$$

The angle, γ_g, between the antenna boresight of the LEO spacecraft and the vector to the deep space Earth station is computed with (21, 22). The LEO spacecraft antenna gain of a typical LEO spacecraft, e.g. EOS, in the direction of the deep space Earth station is computed. The model is a set of straight line segments that approximate the actual pattern [18].

$$\begin{aligned} G_e(\gamma_g) &= -3.5 + 2.5\gamma_g/3 \text{ (dBi)}, && 0° \le \gamma_g < 3° \\ &= 0.091 - 4\gamma_g/11 && , 3° \le \gamma_g < 14° \\ &= -8.5 + 14\gamma_g/56 && , 14° \le \gamma_g < 70° \\ &= 84.25 - 21.5\gamma_g/20 && , 70° \le \gamma_g \text{ c } 90° \\ &= -14.5 && , 90° < \gamma_g \le 180° \end{aligned} \quad (46)$$

The interference power spectral density level at the deep space Earth station receiver is computed.

$$I_o = SD(f) \text{ -1 } P_e + G_e(\gamma_g) \text{ -1 } 1'14 + G_l(\gamma_{rg}) \quad (47)$$

Where

I'_c = LEO transmitter power

Table V shows the simulation results for a population of five LEO spacecraft (2. EOS-1 DB mode, Radarsat-1, SPOT-4, and 111< S-1 [B]). The spacecraft modulators have perfect data waveform symmetry and zero transition time. Statistics of interference to a DSN station are provided on the table. The antenna patterns for the last three spacecraft are the same as the EOS antenna (46) except for additive constants to provide the correct peak antenna gain for each spacecraft. Each interference event is composed of a number of interference samples that occur at 0.5 second intervals. These samples arc plotted on Fig.13 for the simulation. At each sample interval the amount that the interference exceeds the DSN interference criterion [4, 5] is plotted. Some events have only 2 samples (1 second of interference) and some events have up to 14 samples (7 seconds of interference). Interference that is 12 dB and more above the DSN interference criterion frequently occurs,

The effect of 5% data asymmetry on the simulation results is shown in the last column of Table V. The same five spacecraft modulators are used. Fig. 14 shows the interference samples for this simulation. Only the samples that exceed 40 dB are plotted. Interference that is 77 dB and more above the DSN interference criterion frequently occurs.

The antenna pattern of the deep space Earth station that is provided in (45) was developed a number of years ago for generalized Earth stations. More accurate gain data has been made available for the 70 meter antennas of the DSN [19]. This data has been fit with a number of equations.

$$\begin{aligned} G_m(\gamma_{rg}) &= 74.15 - 0.0025\,(2400\gamma_{rg})^2 \text{ (dBi)}, && 0° \le \gamma_{rg} < 0{,}0376° \\ &= 53.7, && 0{,}0376'' \le \gamma_{rg} < 0.04° \\ &= 57.4 - 0{,}025(1350[y,l;-0.049])', && 0.04° < \gamma_{rg} < 0.0626° \\ &= 49, && 0.0626° \le \gamma_{rg} < 0.0905'' \\ &= 25 - 23\log(\gamma_{rg}), && 0.0905° < \gamma_{rg} < 33.2° \\ &= -10 && :33.2°5\ \gamma_{rg} < 180° \end{aligned} \quad (48)$$

Fig.15 contains plots of antenna data, the curve fits from (48), and the ITU pattern [3]. When the computer simulation is run with the curve fits of (48) the percentage of interference to the DSN Earth station is reduced because the ITU pattern overestimates the DSN antenna gain in many regions. However, in the 0.04° to 0.06° region on Fig. 15 the curve fits rise up to 6 dB above the ITU recommended pattern. This would produce interference samples that are frequently 18 dB (6 dB greater than the 12 dB mentioned above) higher than the DSN interference criterion for the case of perfect data

waveform symmetry. When the modulators have .5% data asymmetry, interference samples that are frequently 83 dB (6 dB greater than the 77 dB mentioned above) higher than the 1 DSN criterion would be produced.

All of the simulations use an elevation of 5° and an azimuth of 100° for the deep space Earth station antenna. When larger elevation angles are used, the interference percentages are decreased because the spacecraft spends less time within the same Earth station antenna beamwidth at higher elevations. The simulation results are sensitive to the DSN Earth station latitude, also. As the latitude increases the low Earth orbiter is visible to the Earth station on more orbits. Therefore the interference percentages increase at larger latitudes.

4. Summary and Conclusions

Detailed models of the interference geometry of Earth orbiters and an Earth station are developed. These models allow the accurate determination of antenna gains and path distances. These parameters and the radio system characteristics determine the interference levels at the victim receiver. An example is shown to illustrate the model.

interference from Earth exploration-satellites to a deep space Earth station is simulated. Worst-case levels of power spectral density from low Earth orbiters at a deep space Earth station are computed. These levels exceed the interference criterion of the deep space Earth station in the 8400- to 8450-MHz band. Models are developed to compute the power spectral density of a QPSK signal that has data asymmetry and finite transition time. A simulation of interference from low Earth orbiters to a deep space Earth station is conducted. This simulation computes the path loss and off-axis antenna gains as a function of orbital position of the low Earth orbiter. It can be used to predict the statistics of interference to the deep space Earth station. Table V contains a summary of two different simulations that were performed. Fig. 13 shows the interference samples for the first simulation. Results from the simulation showed that excessive coordination could be avoided if the Earth exploration-satellite spacecraft reduced their emissions by 18 dB in the 8400- to 8450-MHz band for perfect data waveform symmetry. The interference statistics are in close agreement with other simulations [20].

Fig. 14 shows the interference samples for the second simulation. When the modulators have 5% data asymmetry these spacecraft need to reduce the emissions in the MOO- to 8450-MHz band by about 83 dB to avoid excessive coordination. This value is based on the worst case assumption that the discrete interference spectral components are within the 1 DSN receiver bandwidth. Deep space communication systems are especially sensitive to interference. The Earth station receiver has several synchronization loops that track the desired signal components. Interference can cause a loss of lock on these signal components and re-synchronizat ion may take several minutes. During critical mission events it is necessary to transmit and receive scientific data without error or interruption. Loss of signal during these critical times can result in irretrievable data loss.

The models and simulations that arc developed arc sufficientl y general to have application for a variety of problems on the subject of interference prediction.

Acknowledgments

The author gratefully acknowledges the help of Dan Bathker, Benito G.-Luaces, J. Hart (Stanford Telecom), Tien Nguyen, Charles Ruggier, Mike Spencer, and Carroll Winn in the development and testing of the models and simulations and for manuscript review.

The work described in this paper was carried out at the Jet Propulsion Laboratory, California Institute of Technology, under a contract with the National Aeronautics and Space Administration.

References

[1] P. R. Escobal, *Methods of Orbit Determination*. New York: Wiley, 1976.

[2] R. H. Battin, *Introduction to the Mathematics and Methods of Astrodynamics*. New York: American Institute of Aeronautics and Astronautics, 1987.

[3] *International Telecommunication Union Radio Regulations*, ISBN 92-61 -*01221-3, vol. 2*, 1982, Appendix 29, p. AP29-14.

[4] CCIR, "Protection Criteria and Sharing Considerations Relating to Deep-Space Research," *Reports of the CCIR, annex to vol. II, Space Research and Radioastronomy Services*, CCIR Report 685-3, CCIR, Geneva, Switzerland, pp. 281-302, 1990.

[5] CCIR, "Protection Criteria and Sharing Considerations Relating to Deep-Space Research," *Recommendations of the CCIR, vol. II*, Space *Research and Radioastronomy Services*, CCIR Recommendation 578, CCIR, Geneva, Switzerland, p. 12, 1990.

[6] *International Telecommunication Union Radio Regulations*, ISBN 92-61-01221-3, vol. 1, 1982, Article 8, p. RR8-129.

[7] N.F. deGroot, "The Space Frequency Coordination Group," *Telecommunication Journal*, vol. *56*, pp. *238-244*, IV/1989.

[8] SFCG Database, INTA Madrid, Program Version 1.3.

[9] D. Boyd, personal communication, Computer Sciences Corporation, Sterling, Virginia, August 1993.

[10] S. Pasupathy, "Minimum Shift Keying: A Spectral] y Efficient Modulation," IEEE *Communicat ions Society Magazine, pp. 14-22*, July 1979.

[11] B. Tunstall, "Transmit Filtering for EOS Direct Access System Downlink," Memorandum to Jim Scott, Goddard Space Flight Center, July 10, 1992.

[1 2] T.M. Nguyen, "The Impact of NRZ 1 Data Asymmetry on the Performance of a Space Telemetry System," *IEEE Transactions on Electromagnetic Compatibility*, vol. *33*, *pp.* 343-350, November 1991.

[13] S. Haykin, *Communication Systems*, John Wiley & Sons, 1978, ch. 1, p. 15.

[14] B. Sklar, *Digital Communications*, Prentice Hall, 1988, ch. 1, pp. 36-41.

[15] J.K. Holmes, *Coherent Spread Spectrum Systems*, ch. 2., pp. 29-30.

[16] Goddard Space Flight Center, *Tracking and Data Relay Satellite System (TDRSS) User's Guide*, Greenbelt, Maryland, STDN No. 101.2, Rev. 5, p. 3-124, Sep. 1984.

[17] *Reference Data for Radio Engineers*, New York: Howard W. Sams & Co., Inc., 1982, ch. 33, p. 33-11,12,

[18] J. Hart, "interference Analysis for EOS AM Direct Access System," Memorandum of Stanford Telecom, July 7, 1992.

[19] *D.* Bathker, personal communication, Jet Propulsion Laboratory, Pasadena, CA, July 1993.

[20] J. Hart, "Compliance of EOS Direct Access System with DSN Protection Criteria," Interoffice Memorandum (internal document), Stanford Telecom, Seabrook, Maryland, May 17, 1993.

Table I Near-Earth Spacecraft that Transmit in the 8025- to 8400-MHz Band

Spacecraft Frequency (MHz)	Transmitter Power (dBW)	Peak Antenna Gain (dBi)	Modulation/ Tots! Output Symbol Rate (MSPS)	Minimum Orbit Altitude (km)/Inclination (deg)
CBERS/8212.5	13.6	5.5	QPSK/53	760.5 /98.5
EOS (DB)/8212.5	11.8 (4.8 -1, ?0.8 -Q)	7	UQPSK/30 -1,30- Q	705/98.2
EOS (DD)/8212.5	11.8 (4.8 -1, 10.8 -Q)	7	UQPSK/30 . I, 210 . Q	705/98.2
EOS (DP)/8212.5	11.S (8.8 I, 8.8 - Q)	7	QPSK/300	705/98.2
ERS-1(A)/8040	11.5	5	QPSK/15	7s5/9s.5
ERS-1(B)/8140	11.5	5	QPSK/105	7s5/9s.5
IRS-1B/8316	13	6.5	QPSK/20.8	900/99.0
Landsat-6/8342.5	-1.9	26.2	BPSK/85	705/98.2
MOS-1B/8350	6	4.3	MSK/8.78	909/99.0
ENVISAT/8200	9	8	QPSK/100	850/98.5
Radarsat-1/8230	11	6	QPSK/105	7S9/9S.6
SPOT-1 /S253	12	6.4	QPSK/49.372	S22/9S.7
SPOT-4 /8253	12	5.4	QPSK/49.372	S22/9S.7
SSIPR/8320	11.s	6	/64	630/9s.5

Table 11 Spectral Density Equations

Modulation	Spectral Density (Baseband)*
QPSK	$(2/SR)[\sin(2\pi f/SR)]^2/(2\pi f/SR)^2$
UQPSK	$(r_I/SR_I)[\sin(\pi f/SR_I)]^2/(\pi f/SR_I)^2 + (r_Q/SR_Q)[\sin(\pi f/SR_Q)]^2/(\pi f/SR_Q)^2$
PSK	$(1/SR)[\sin(\pi f/SR)]^2/(\pi f/SR)^2$
MSK	$[16/(\pi^2 SR)][\cos(2\pi f/SR)]^2/(1-16f^2/SR^2)^2$

QPSK - Quadriphase-Shift Keying
UQPSK - Unbalanced Quadriphase-Shift Keying
PSK - Phase-Shift Keying
MSK - Minimum-Shift Keying

SR = total output symbol rate
f = frequency
r_I = ratio of power in I channel to total power
SR_I = symbol rate of I channel
r_Q = ratio of power in Q channel to total power
SR_Q = symbol rate of Q channel

• Replace "f" with "f-fC" (where f_c is the center frequency) to obtain the spectral density at the center frequency

Table III Adjacent Band Spacecraft That Exceed the DSN Interference Criterion

Spacecraft designator	Magnitude by which S400 MHz band Allowable Interference is exceeded, (dB)			
	Ideal Data Waveform	0.05% Data Asymmetry	0.5% Data Asymmetry	5% Data Asymmetry
CBERS	45	76	915	103
EOS DE mode	45	76	96	107
EOS DD mode	43			
EOSDP mode	51	51"	51'	51"
ERS-1(A)	29	73	89	88
ERS-1(B)	40	73	93	109
IRS-1B	46	75	95	9s
Landsat-6	64	82	102	121
ENVISAT	43	73	93	110
Radarsat-1	46	73	93	111
SPOT-1	45	74	94	108
SPOT-4	4s	73	93	111
SSIPR	53	76	96	114

* For this spacecraft/mode no discrete component spectral lines fall within the deep space band (8.40-8.45 GHz).

Table V Simulation Results for Interference to a Deep Space Earth Station

Parameter	Perfect Data Waveform Symmetry	5% Data Asymmetry
Duration of Simulation (years)	1	1
Sample Interval (seconds)	0.5	5
Interference Events	108	8973
Interference Samples	996	1.398×10^{6}
Interference Percentage	1.6×10^{-3}	22,2
Interference Duration		
Shortest	1.00 seconds	0.08 minutes
Longest	7.00 seconds	27,92 minutes
Average	4.61 seconds	12.29 minutes
Time Between Interference Events		
Shortest	0.07 days	0.17 minutes
Longest	14.03 days	111 minutes
Average	3.38 days	46,37 minutes

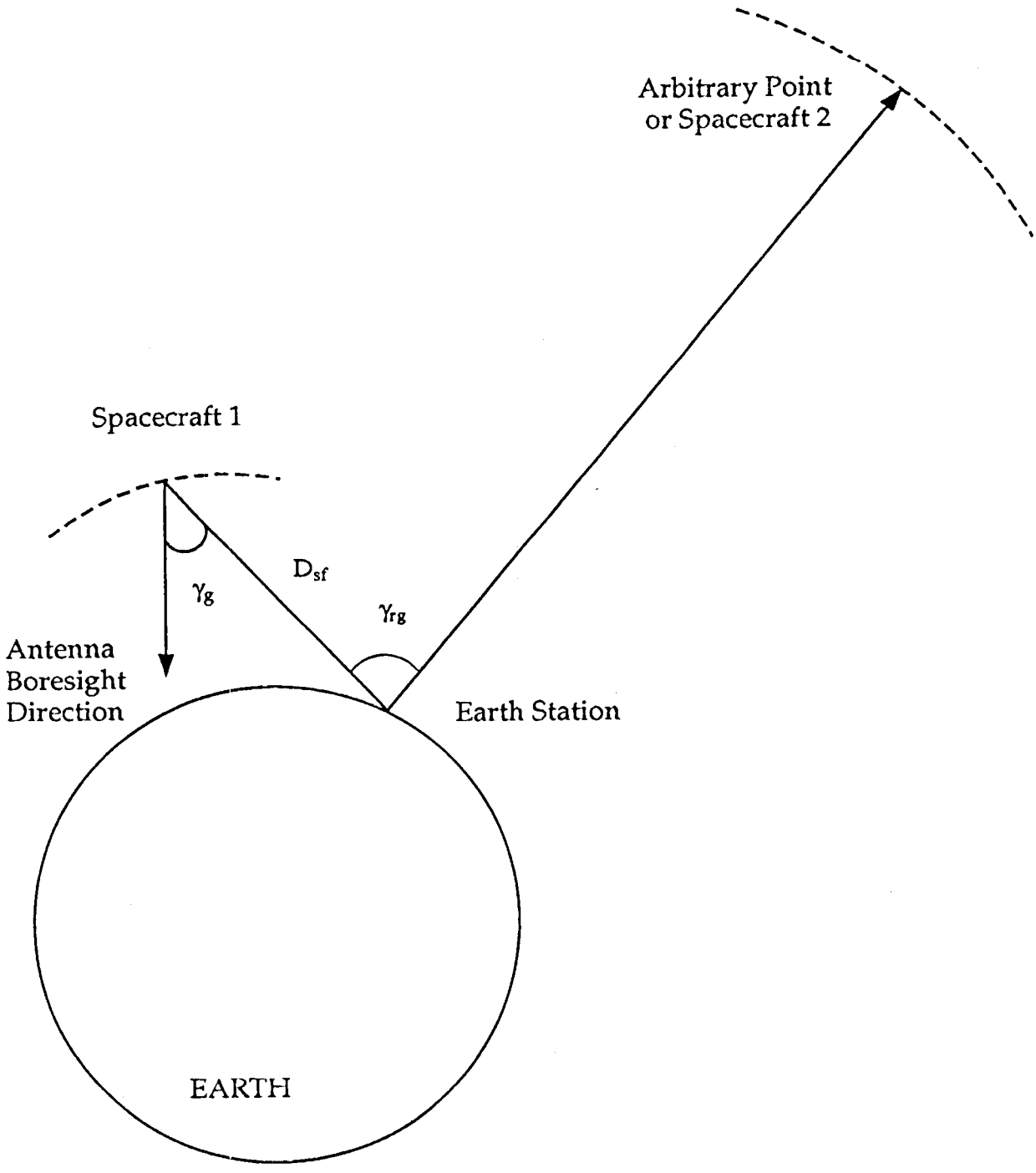

Fig. l. Interference geometry for Earth orbiters and an Earth station.

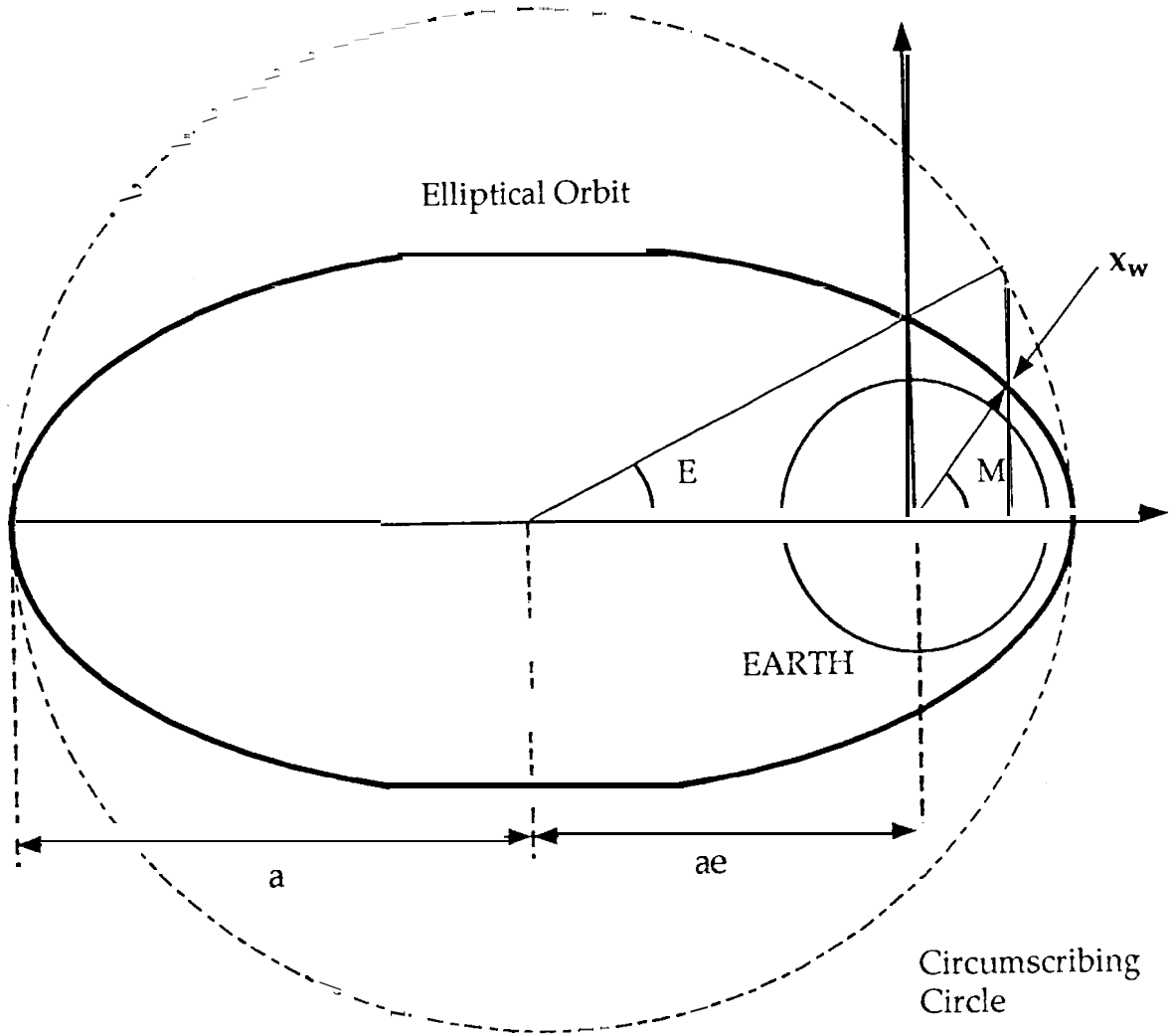

Fig. 2. Spacecraft orbit plane geometry.

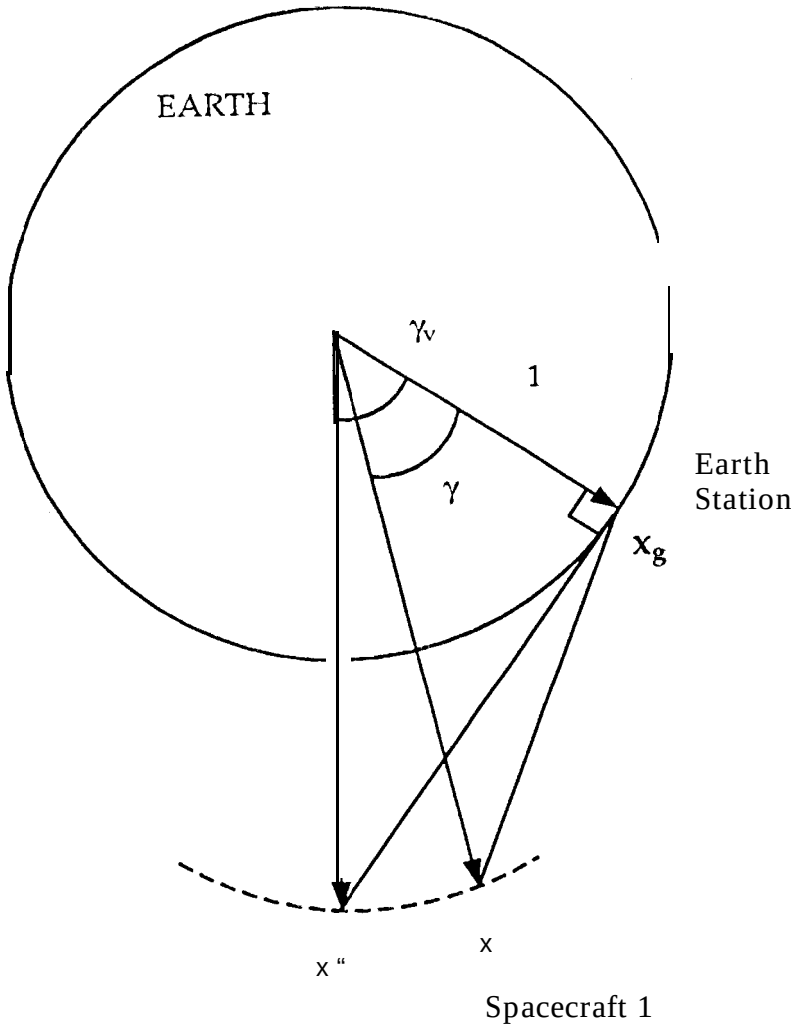

Fig. **3,** Visibility between a spacecraft and an Earth station,

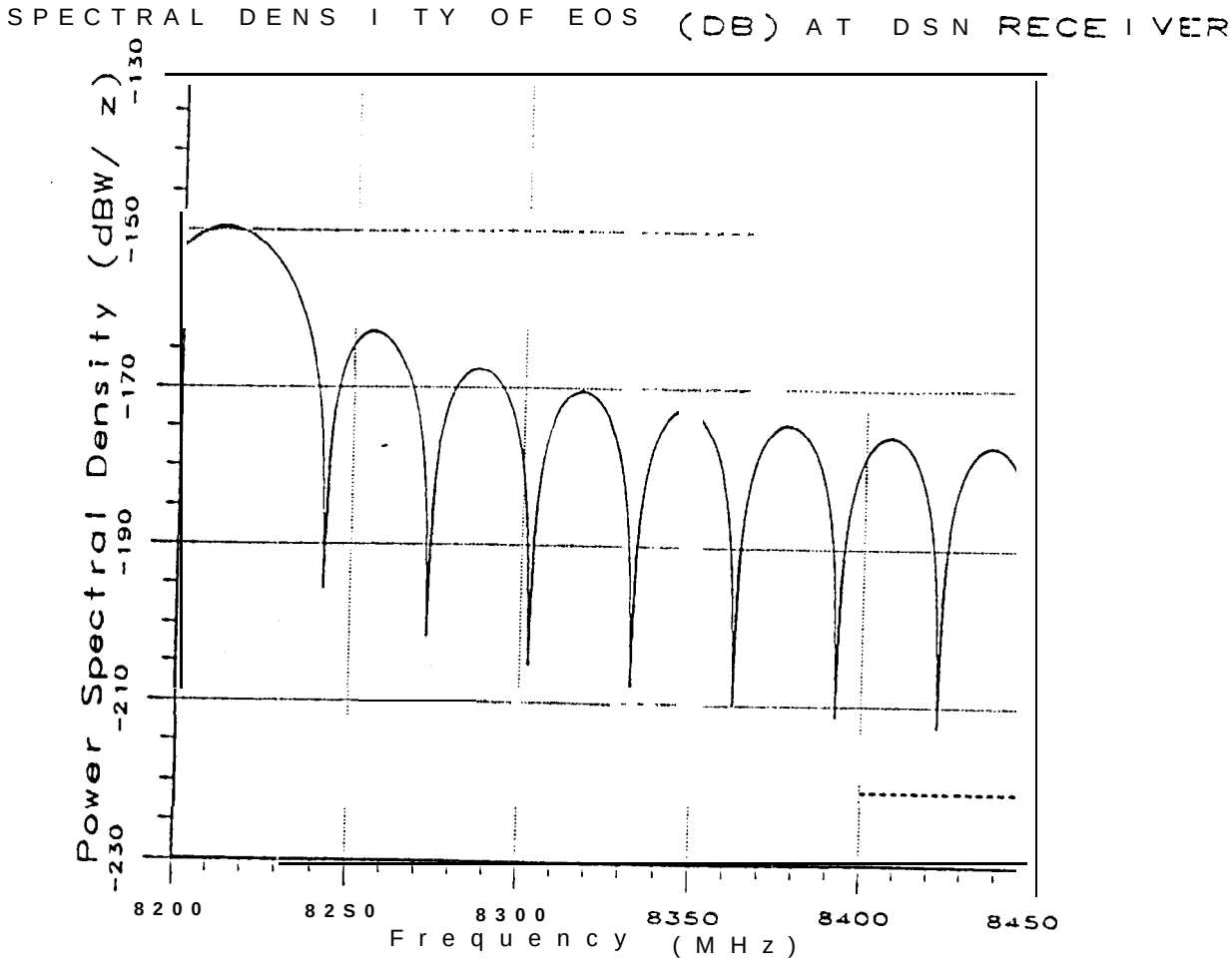

Fig. 4. Spectral density of EOS (DB mode) at DSN receiver.

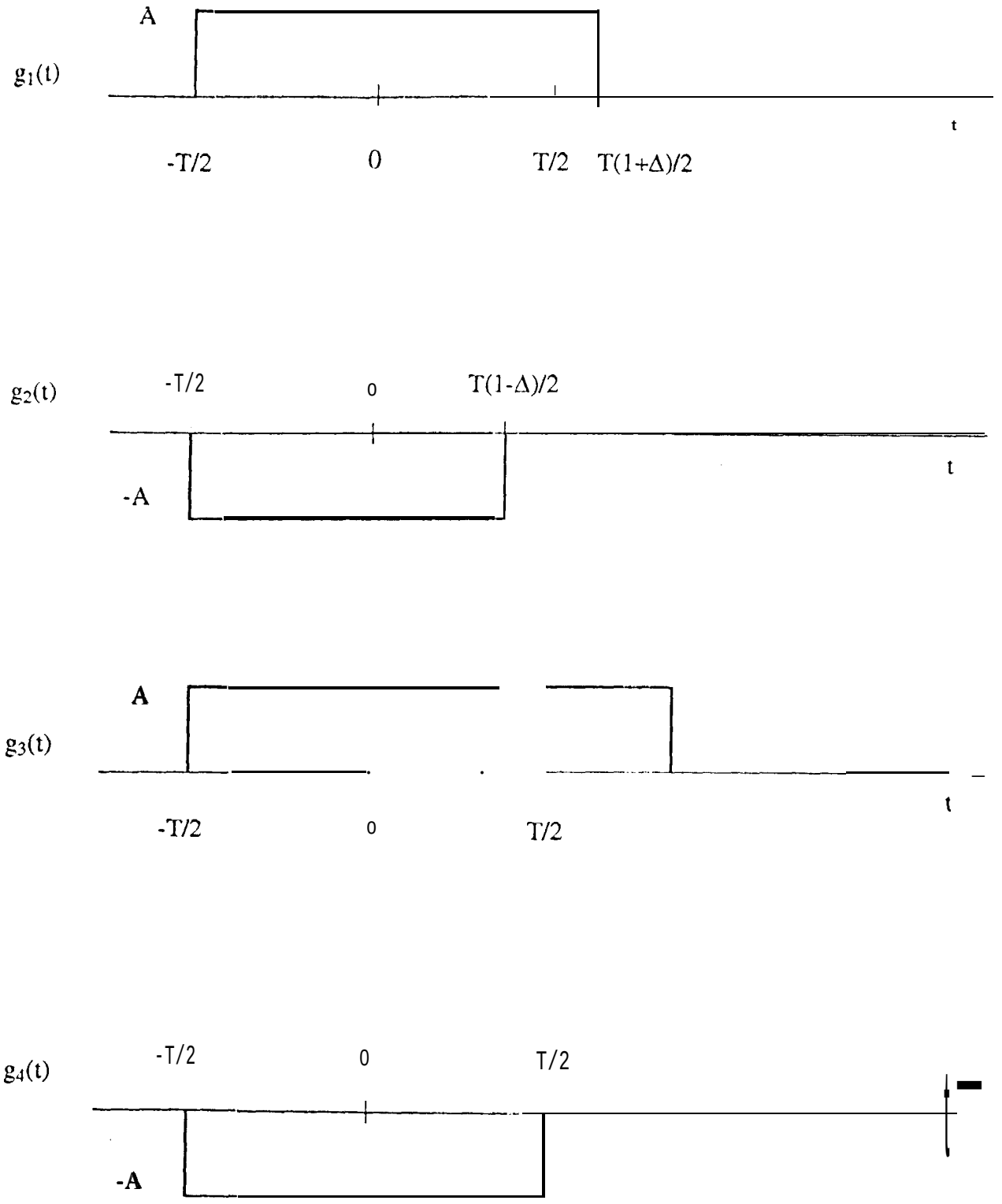

Fig. 5. Baseband 4-ary source model for NRZ data asymmetry,

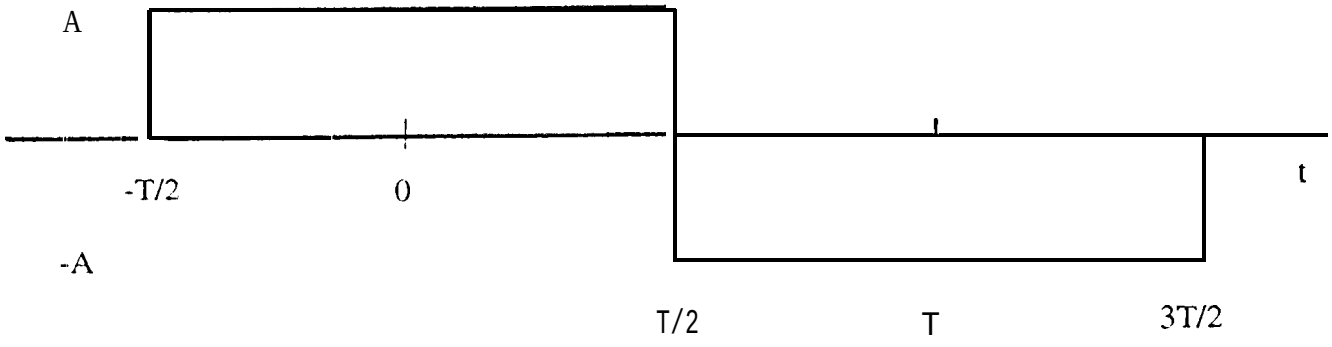

PERFECT TRANSITION
(filter input)

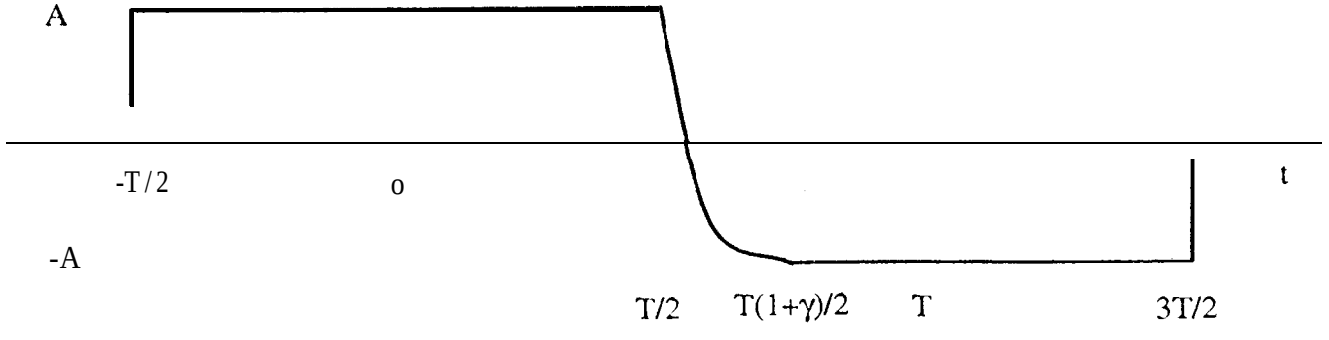

FINITE TRANSITION
(filter output)

Fig. **6.** Model for finite transition time.

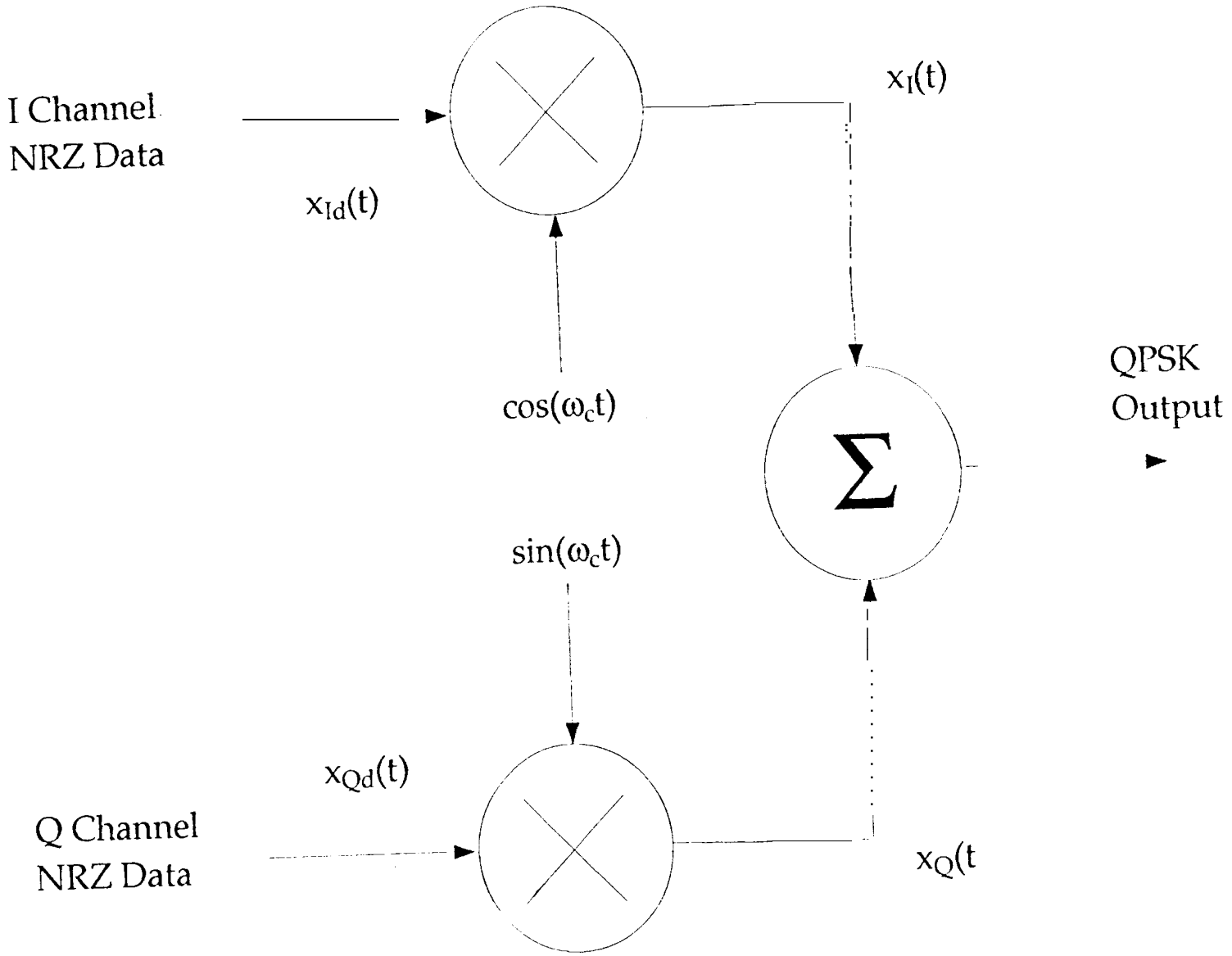

Fig. 7. QPSK Modulator

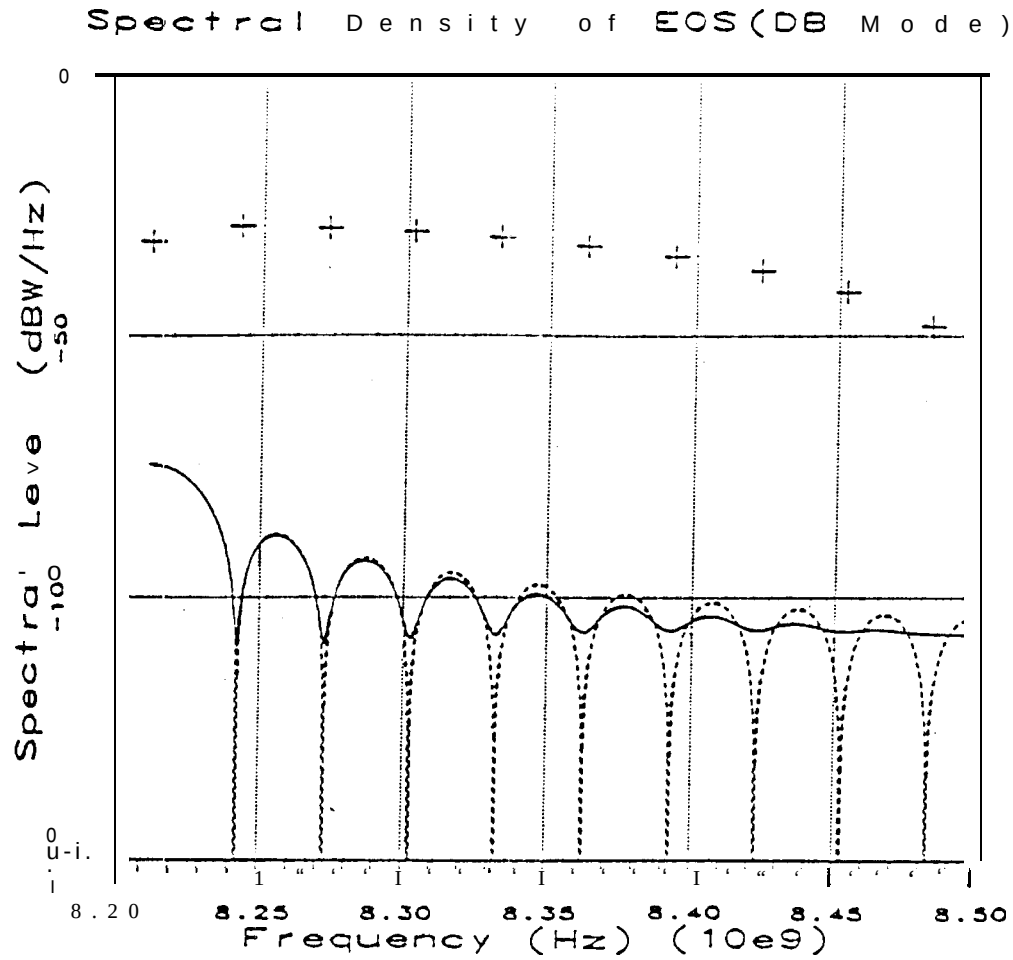

Fig. 8. Power spectral density of EOS (5% data asymmetry).

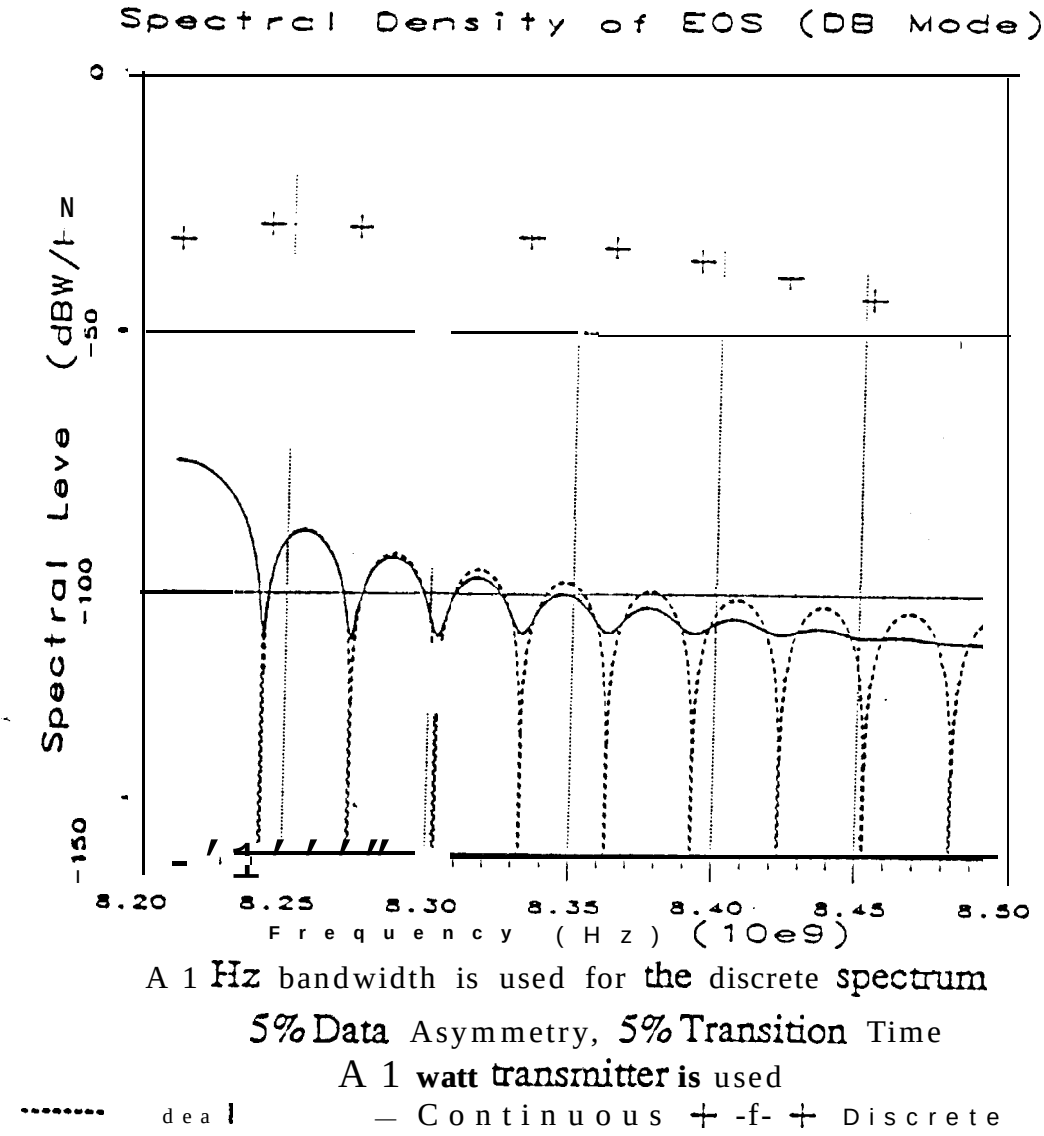

Fig. 9. Power spectral density of EOS (5% data asymmetry, 5% transition time),

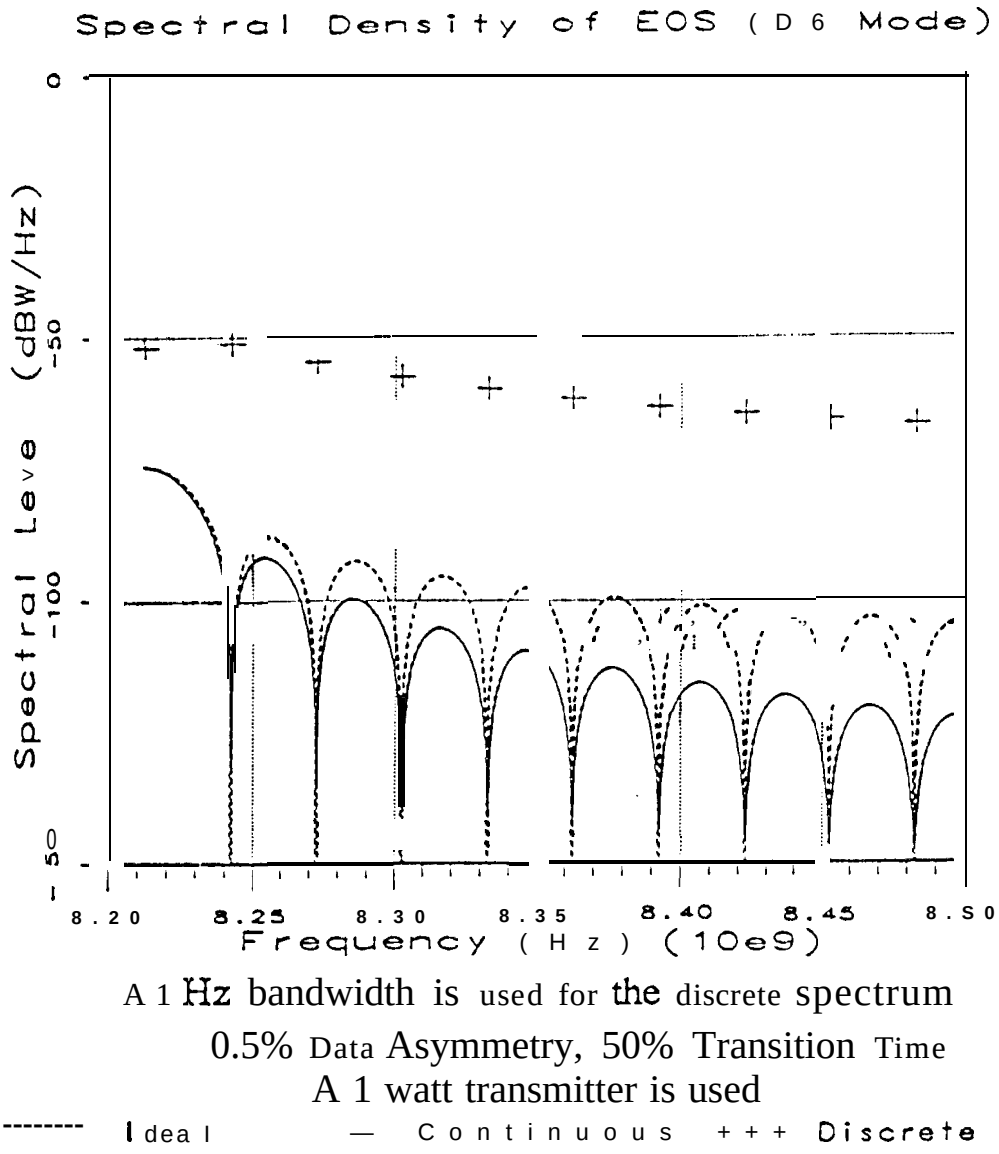

Fig. 10. Powers spectral density of EOS (0.5% data asymmetry, 50% transition time).

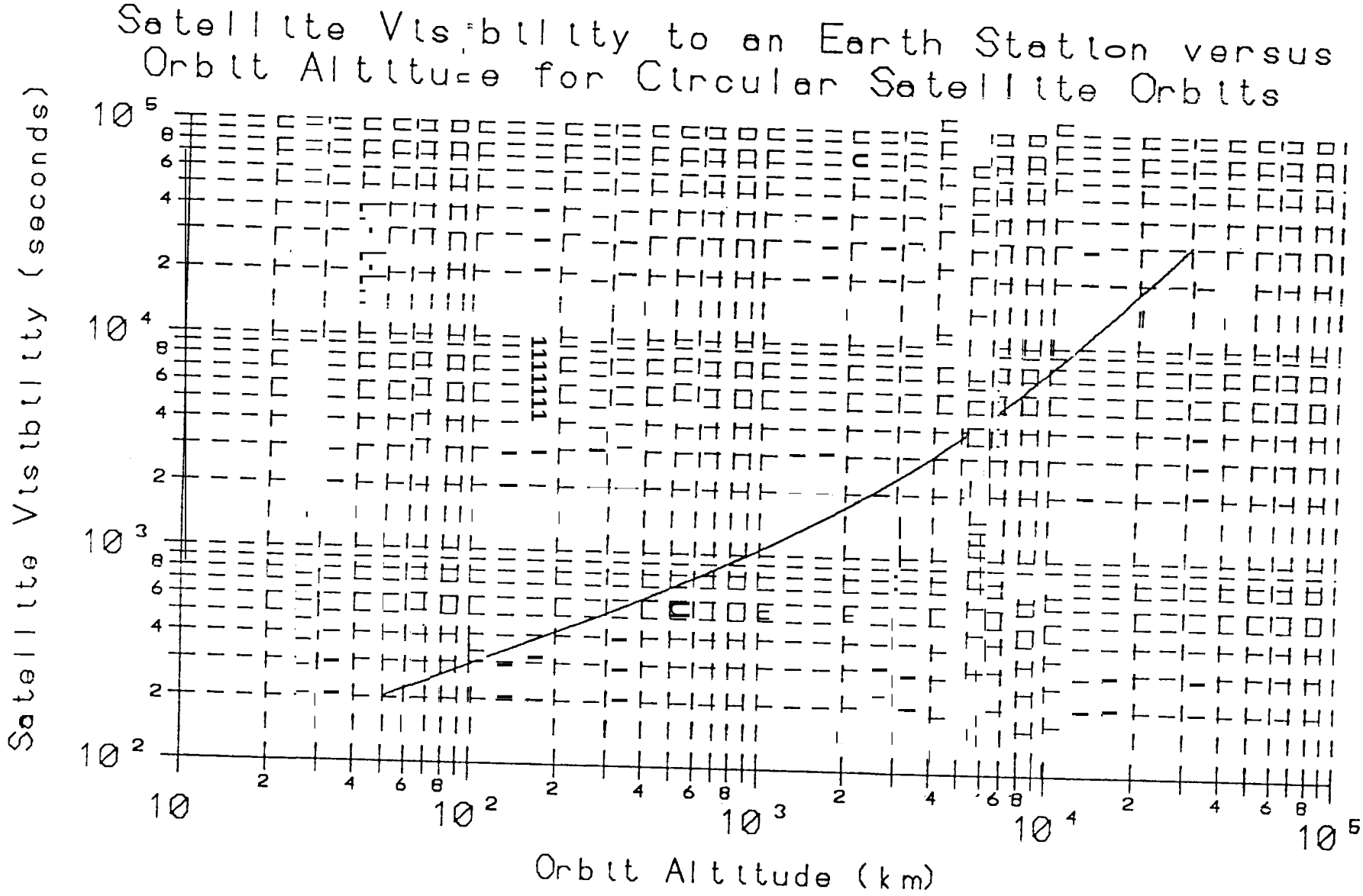

Fig. 11. Satelli e visibility an Earth s ation versus orbit altitude for circular satellite orbits.

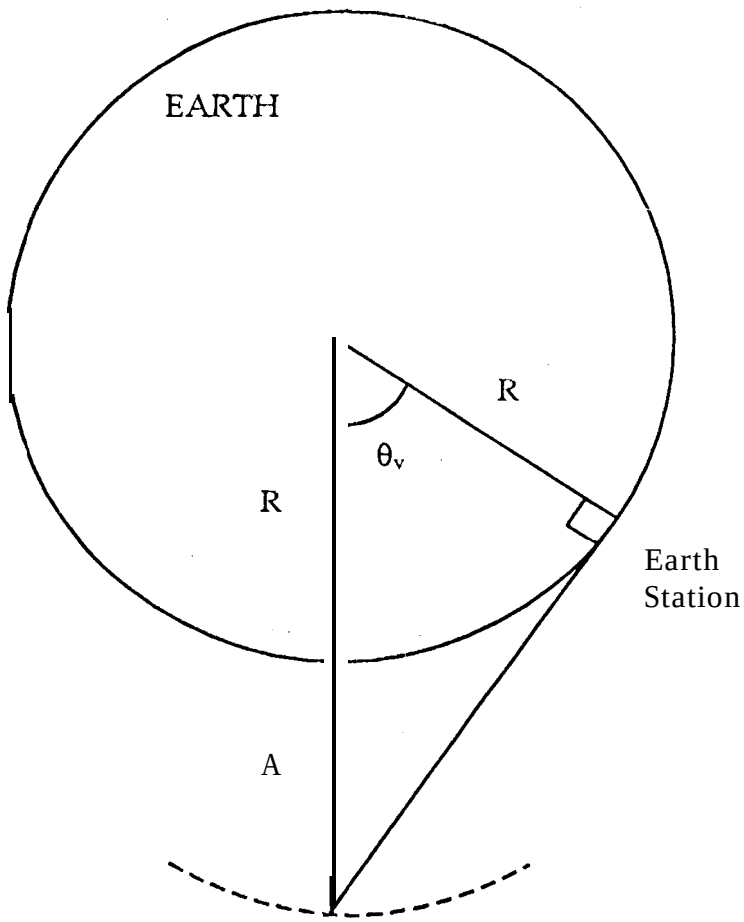

Fig. 12. Geometry for spacecraft visibility time calculation.

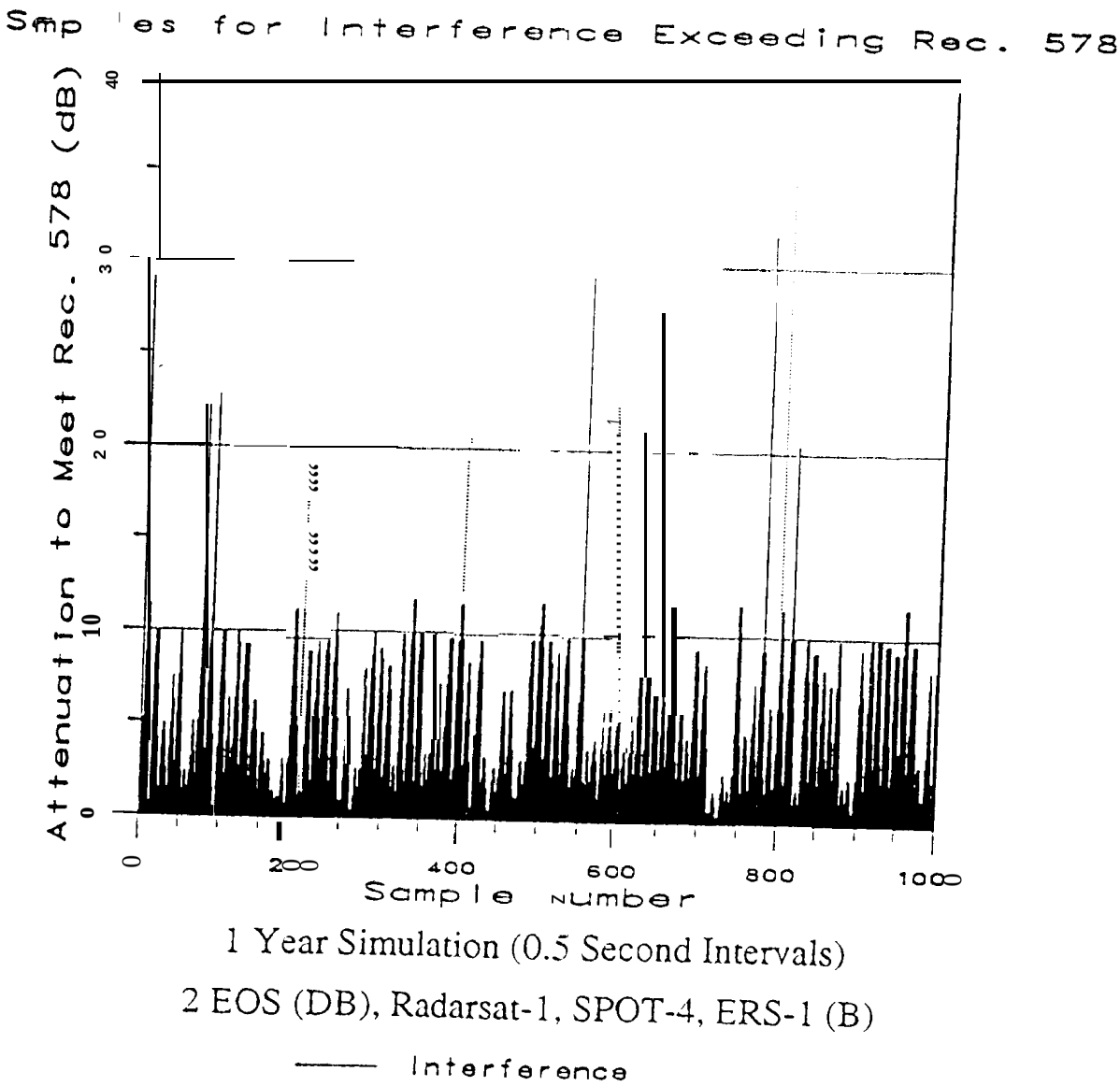

Fig. 13. Interference samples for 5 spacecraft with perfec data waveform symmetry.

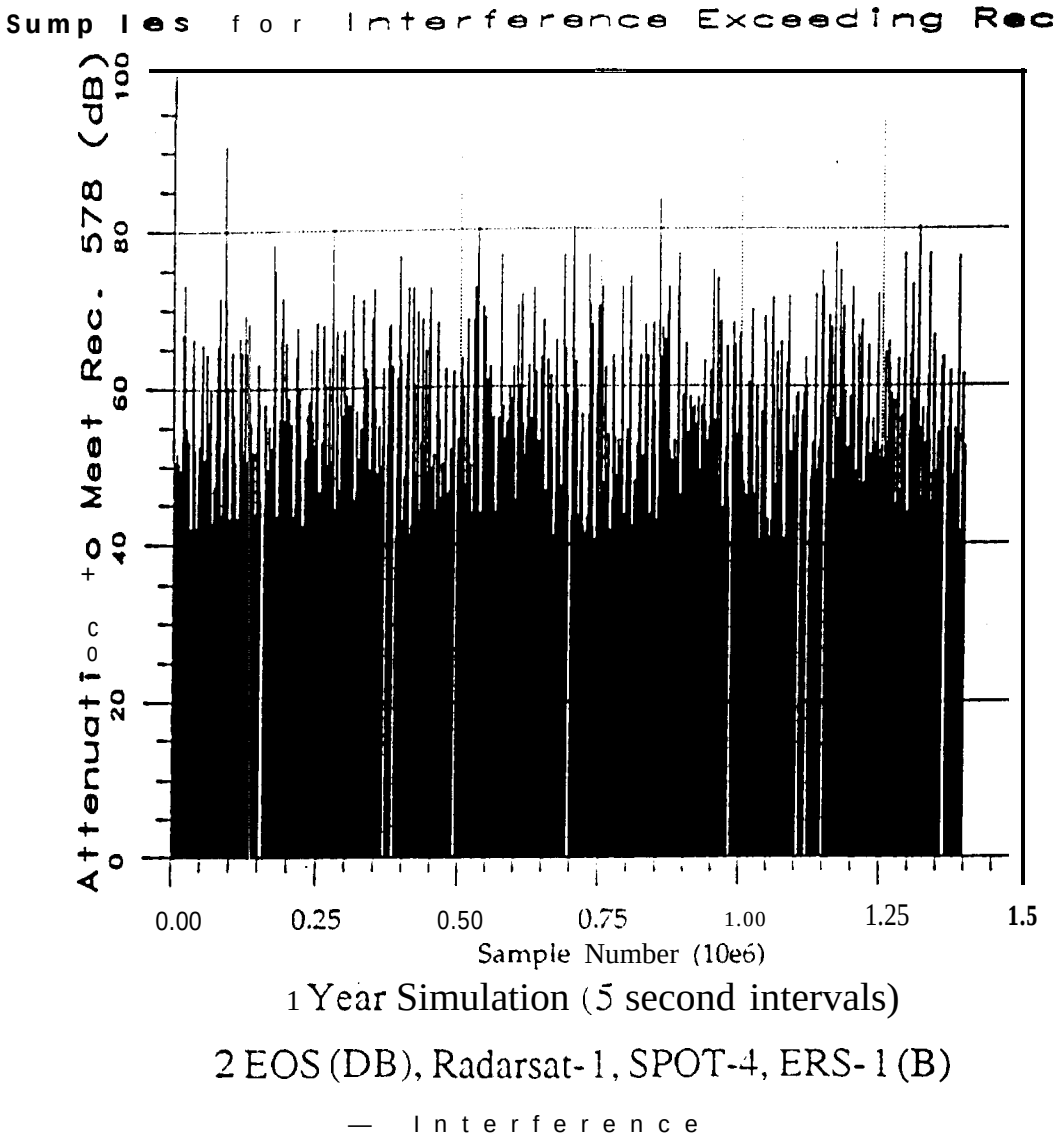

Fig. 14. Interference samples for 5 spacecraft with 5% data asymmetry

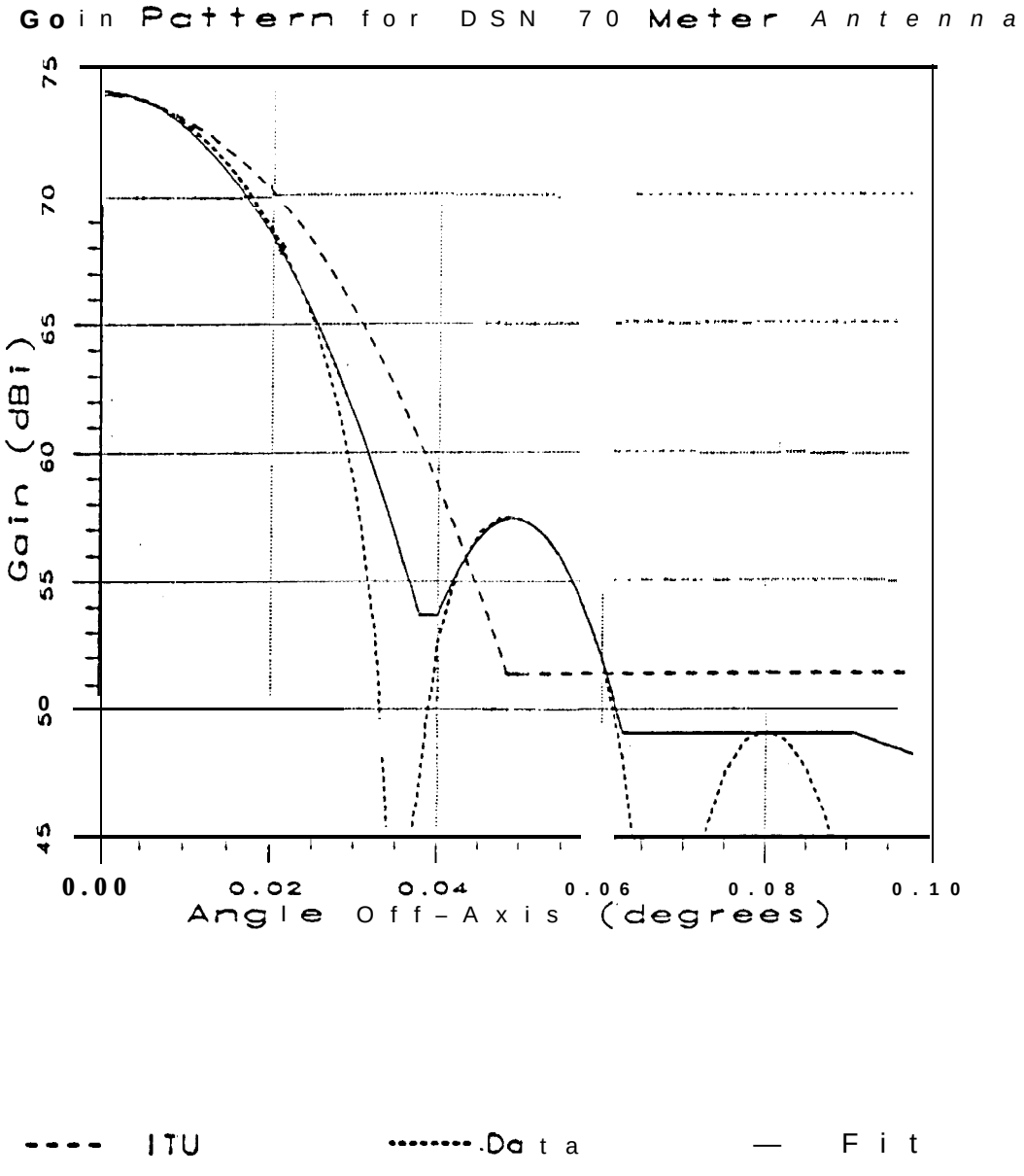

Fig. 15. Gain pattern for DSN 70 meter antenna.